

Spectral Properties of $[(\text{Ni}_{0.45}\text{Co}_{0.2}\text{Zn}_{0.35}\text{F}_2\text{O}_4)_{1-x}(\text{Sodium Acetylacetonate})_x]$ Nanocomposite

O. M. Hemeda¹, A. Tawfik¹, D. E. El Refaey², Adly H. El-Sayed³, Sh. Mohamed⁴

¹Department of Physics, Faculty of Science, Tanta University, Tanta, Egypt

²Department of Physics, Faculty of Science, Suez University, Suez, Egypt

³Department of Physics, Faculty of Science, Alexandria University, Alexandria, Egypt

⁴Department of Physics, Faculty of Science, El-Qassim University, El-Qassim, Saudi Arabia

Email: nano_physics@yahoo.com

How to cite this paper: Hemeda, O.M., Tawfik, A., El Refaey, D.E., El-Sayed, A.H. and Mohamed, Sh. (2017) Spectral Properties of $[(\text{Ni}_{0.45}\text{Co}_{0.2}\text{Zn}_{0.35}\text{F}_2\text{O}_4)_{1-x}(\text{Sodium Acetylacetonate})_x]$ Nanocomposite. *Open Journal of Applied Sciences*, 7, 15-30. <http://dx.doi.org/10.4236/ojapps.2017.71002>

Received: November 6, 2016

Accepted: January 22, 2017

Published: January 25, 2017

Copyright © 2017 by authors and Scientific Research Publishing Inc. This work is licensed under the Creative Commons Attribution International License (CC BY 4.0).

<http://creativecommons.org/licenses/by/4.0/>



Open Access

Abstract

The pure spinel phase of $\text{Ni}_{0.45}\text{Co}_{0.2}\text{Zn}_{0.35}\text{F}_2\text{O}_4$ was prepared by coprecipitation method and ceramic method. The nanocomposite $[(\text{NCZF})_{1-x}(\text{Na}(\text{ac.ac}))_x]$ ($x = 0\%$, 20% , 40% , 60% , 80% , 100%) was prepared by mixing two phases, $\text{Ni}_{0.45}\text{Co}_{0.2}\text{Zn}_{0.35}\text{F}_2\text{O}_4$ with coprecipitation method [NCZF] and sodium acetylacetonate [Na(ac.ac)]. The TEM photographs of the as prepared ferrite samples by coprecipitation method at different ratios of Na(ac.ac) show that the crystalline cubic nanoparticles diameter were ranged from 26 - 36 nm and the particle size of Na(ac.ac) is greater than NCZF. The same behavior has also confirmed by XRD patterns indicating polycrystalline nature of prepared sample. The comparison between the SEM micrographs for NCZF nanoparticles prepared by a) ceramic method and b) co-precipitation method was done to show the effect of preparation condition on the microstructure. IR analysis confirms the composites formation.

Keywords

Spectral Properties, Nanocomposite, SEM, TEM, IR

1. Introduction

Recently, increasing developments in the electronics industry, electronic components have been required with smaller size, higher performance, and multi-function capability. Therefore, composites, especially ferromagnetic-ferroelectric composites, have been attracting more and more attention [1] [2] [3] [4]. When ferromagnetic and ferroelectric phase coexist in one material, novel properties, such as magneto-electric and magneto-optic properties, are expected due to the interaction between magnetization and electric polarization. Therefore, much

work on ferromagnetic-ferroelectric composites has been carried out. From history and development of magnetoelectric phenomenon (ME), the coupling between electric and magnetic fields was initially discovered by Rontgen in 1888 [5] when he found that a moving dielectric placed in an electric field has become magnetized, and then was theoretically described by Curie in 1894 [6] on the base of crystal symmetry considerations. The discovery of the phenomenon of ferroelectricity was made by Valasek in 1920 [7]. Fox and Scott [8] have also shown that ferroelectricity can produce magnetic order and vice versa. This has provoked interest in study and understanding of “multiferroics” and “magnetoelectric” materials. However, many reports indicate that the introduction of low-dielectric-constant (ϵ) ferrite and the defect reaction between the ferrite and ferroelectric phases would result in a low dielectric constant for the composite, which is not compatible with the trend for higher capacitance and smaller size for electronic components [3]. On the other hand, according to percolation theory, the dielectric constant depends strongly on the conductivity ratio of the ferroelectric and ferrite phases [9] [10]. A higher dielectric constant can be obtained by increasing the conductivity of the ferrite phase, especially for composites with a ferrite volume fraction in the neighborhood of the percolation threshold. As is well known, the conductivity of ferrites, such as $(\text{Ni}, \text{Zn})\text{Fe}_{2+x}\text{O}_4$, is tunable by adjusting the value of x . Fe-rich ferrite ($x > 0$) has higher conductivity because of electron hopping between Fe^{+3} and Fe^{+2} . This implies that a ferromagnetic-ferroelectric composite with a high dielectric constant can be fabricated by introducing Fe-rich ferrite fillers into a ferroelectric matrix of high resistance.

2. Experimental

2.1. Sample Preparation

2.1.1. Ferrite Preparation with Ceramic Method

In the present investigation sample, having $\text{Ni}_{0.45}\text{Co}_{0.2}\text{Zn}_{0.35}\text{Fe}_2\text{O}_4$ structure was prepared. The starting materials were NiO, CoO, ZnO, and Fe_2O_3 . All materials used were of highly chemically pure grade (99.99%), suitable proportions of these starting materials (oxides) were weighed by using a digital balance type (OHAUS B 100) as shown in **Table 1**.

Then, all oxides were grinded in an agate mortar in order to obtain very fine powder and then mixed thoroughly in presence of distilled water to improve the homogeneity using a retch ball mix. The resulting mixture was calcined in air for 4 h at 950°C , then the calcined products were well grinded again in order to obtain fine powder. The fine powder was pressed at room temperature in the form of discs and triodes at constant pressure of 8 kp/cm^2 in stainless steel mold. The

Table 1. The weights of starting material, NiO, CoO, ZnO, and Fe_2O_3 , in gram for $\text{Ni}_{0.45}\text{Co}_{0.2}\text{Zn}_{0.35}\text{Fe}_2\text{O}_4$.

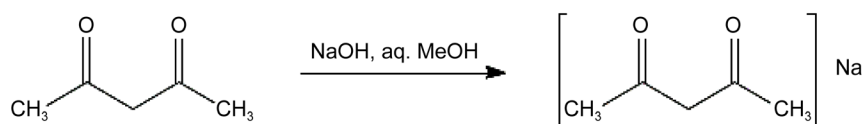
The composition	Weight of mixed oxides in grams			
	NiO	CoO	ZnO	Fe_2O_4
$\text{Ni}_{0.45}\text{Co}_{0.2}\text{Zn}_{0.35}\text{Fe}_2\text{O}_4$	6.7238	2.9973	5.6965	31.9384

samples finally sintered at 1100 °k for 5 hour in air and then left to cool gradually inside the electric furnace. The samples were polished to obtain discs with two uniform parallel surface. Contacts on the sample surface were made by silver paste.

2.1.2. Ferrite Preparation with Co-Precipitation Method

$\text{Ni}_{0.45}\text{Co}_{0.2}\text{Zn}_{0.35}\text{Fe}_2\text{O}_4$ ferrite particles was prepared by chemical precipitation of $[\text{NiCl}_2, \text{CoCl}_2, \text{ZnCl}_2]$ and $[\text{FeCl}_3]$ (1:2 molar ratio) by addition 25% ammonia solution [11]. The volume of reaction mixture have been mixed using magnetic stirring during continuous slow addition of 25 ml ammonia solution and the heating continued for thirty minutes. The powder precipitate was decanted in and washed with 500 ml distilled water [12].

2.1.3. Preparation of Sodium Acetylacetonate



Sodium acetylacetonate is prepared by dissolving 40 g (1 mole) of sodium hydroxide in 50 ml of water and adding to this 200 ml of methanol. This solution is added, slowly with hand stirring, to 100 g (1 mole) of acetylacetone contained in a 500-ml flask. The creamy-white crystalline salt separates from solution immediately. The flask is stoppered and cooled in ice (or in a refrigerator) for 2 hours or overnight. The sodium salt is collected on a Büchner funnel and washed with two small portions of cold methanol. After the salt is air dried, it is dried further either by allowing it to stand in a vacuum desiccator at room temperature or by heating it in a vacuum oven at 100° for 3 hours. The anhydrous product is stable and can be stored indefinitely in a stoppered jar [13].

2.1.4. Preparation of the Composites

$\text{Ni}_{0.45}\text{Co}_{0.2}\text{Zn}_{0.35}\text{Fe}_3\text{O}_4$ [NCZF] and Sodium Acetylacetonate $[\text{Na}(\text{acac})]$ were mixed with the percentage according to formula $[(\text{NCZF})_{1-x}(\text{Na}(\text{ac.ac}))_x]$, ($x = 0\%, 20\%, 40\%, 60\%, 80\%, 100\%$). The composites were mixed and ground very well for 12 hours using agent mortar. Finally, all samples were ground and pressed at room temperature into tablets under of 10 Tonn/cm² of diameter 1cm and 0.4 cm thickness.

2.2. Experimental Processes

XRD - TEM - SEM - IR Spectroscopy.

3. Results and Discussion

3.1. X-Ray Diffraction Pattern

Figure 1(a) shows the diffraction pattern of pure spinel phase of $\text{Ni}_{0.45}\text{Co}_{0.2}\text{Zn}_{0.35}\text{Fe}_2\text{O}_4$ [NCZF] prepared by co-precipitation method and ceramic method whereas

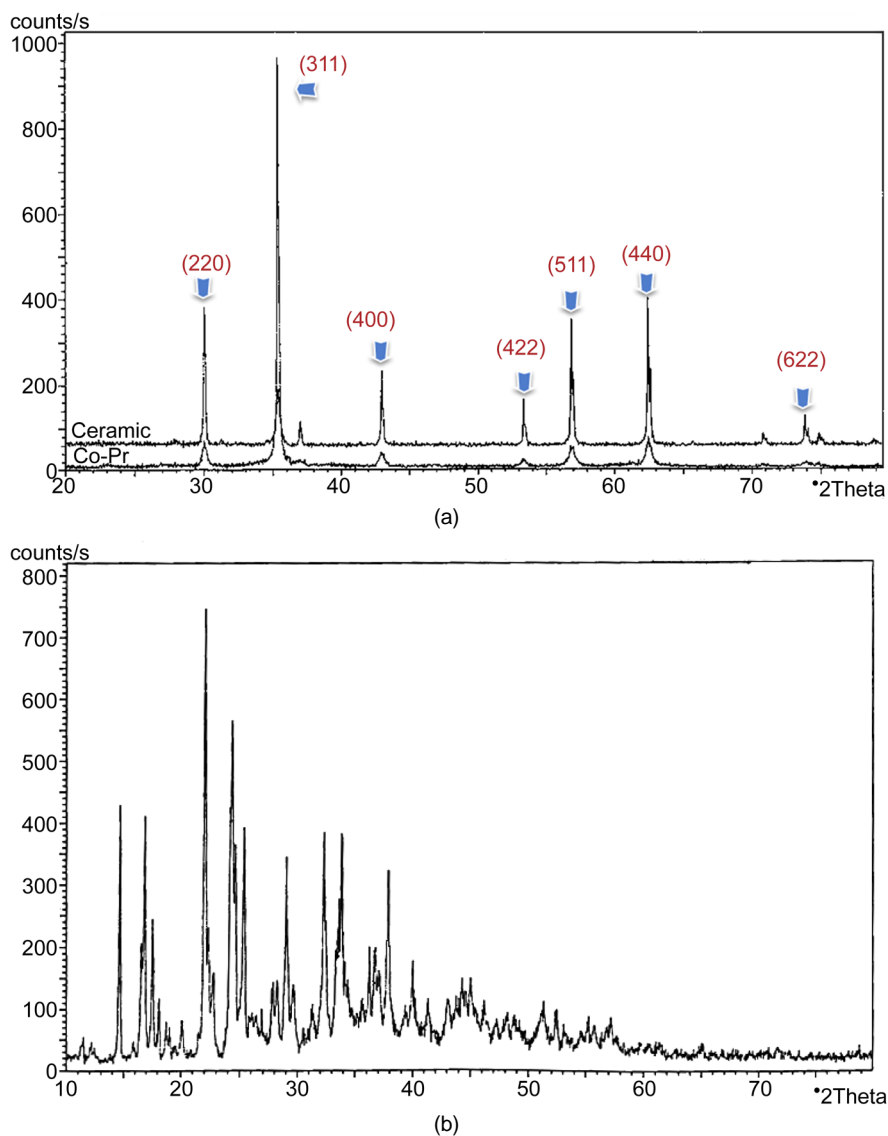


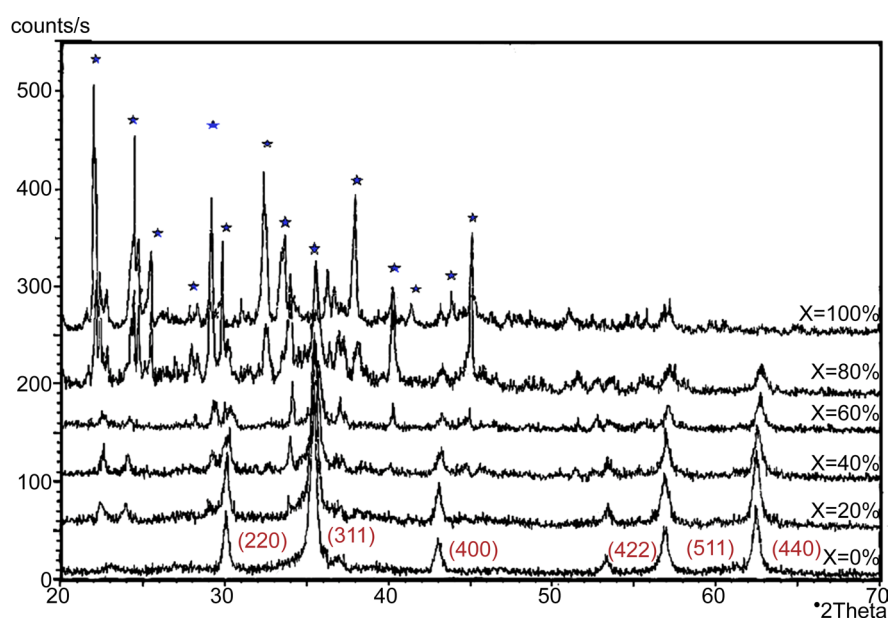
Figure 1. (a) Comparison between XRD of pure NCZF ferrite preparation by ceramic method and co-precipitation method; (b) XRD pattern characteristic the Na(ac.ac).

Figure 1(b) shows the different pattern of Na(ac.ac). All peaks were found to be in good agreement with that obtained by JCPDS card. The d-spacing for as prepared pure Na(ac.ac) were calculated and agreed with that of published Na(ac.ac) as shown in **Table 2**. Peak intensity is given at $2\theta = 22.01^\circ$, the other stronger diffraction peak 16.9° , 17.55° , 24.5° were in agreement with previous work for (Na(ac.ac)). The XRD of nanocomposite in **Figure 2** is showed that the addition (Na(ac.ac)) has considerable effect on crystalline morphology structure of both ferrite and (Na(ac.ac)) [14] [15].

The ferrite diffraction peaks intensity decrease by increasing (Na(ac.ac)) ratio. The (XRD) diffractogram of the composite showed broad peaks because of the presence of nanoparticles. The changes occurred at peak intensities for the two phases indicates the interaction between ferrimagnetic and ferroelectric phases, and the formation of composite with two phases.

Table 2. Diffraction pattern of ferroelectric phase (Na(ac.ac)).

2 θ °	Previous data (*), (**)	Present work
	d(A)°	d(A)°
16.90	4.83842	4.83842
17.55	2.96446	2.96446
22.01	2.52808	2.52808
24.50	2.42134	2.42134
29.01	2.09698	2.09698
32.29	2.03174	2.03174
33.8	1.93811	1.93811
37.85	1.61423	1.61423
44.30	1.4831	1.4831

**Figure 2.** XRD for $[(\text{Ni}_{0.45}\text{Co}_{0.2}\text{Zn}_{0.35}\text{Fe}_2\text{O}_4)_{x-1} + \text{N}(\text{acac})_x]$, $x = 0\%$, 20% , 40% , 60% , 80% , 100% .

The XRD patterns were used to estimate the crystallite size from the most intense peaks using Scherer's equation [16]

$$t = \frac{K\lambda}{h_{1/2} \cos \theta}$$

where

- $K = 0.89$ is Scherer constant.
- $h_{1/2}$ is the full width at half maximum, intensity of X-ray diffraction.
- λ is the wave length of the X-ray for $\text{CuK}\alpha$ radiation (1.541178\AA), and
- θ is angle of diffraction in radial.

The calculated average crystallite size was found 25 - 30 nm for ferrimagnetic phase and from 47 - 52 nm for ferroelectric phase. The dependence of crystallite

size for both phases on Na(ac.ac) content is shown in **Figure 3**.

The average crystallite size of both phases increase by increasing Na(ac.ac) content whereas the value of crystallite size of Na(ac.ac) is higher than that of ferrite phase. The presences of Na(ac.ac) improve the crystalline state of the samples which lead to the increase of crystalline size. The calculated lattice Constance (a) as a function of Na(ac.ac) content for ferrimagnetic phase shown in **Figure 4**, which show that, there is increase of the Lattice constant by increasing Na(ac.ac) content up to 0.4 and then decreases. The increase of lattice constant may be due to the expansion of unit cell because the presence of Na(ac.ac) increases of internal strain in the composite. After certain limit the Na(ac.ac) phase precipitates at grain boundaries and prevent the ferrite phase from expansion, leading to decrease the crystallite size.

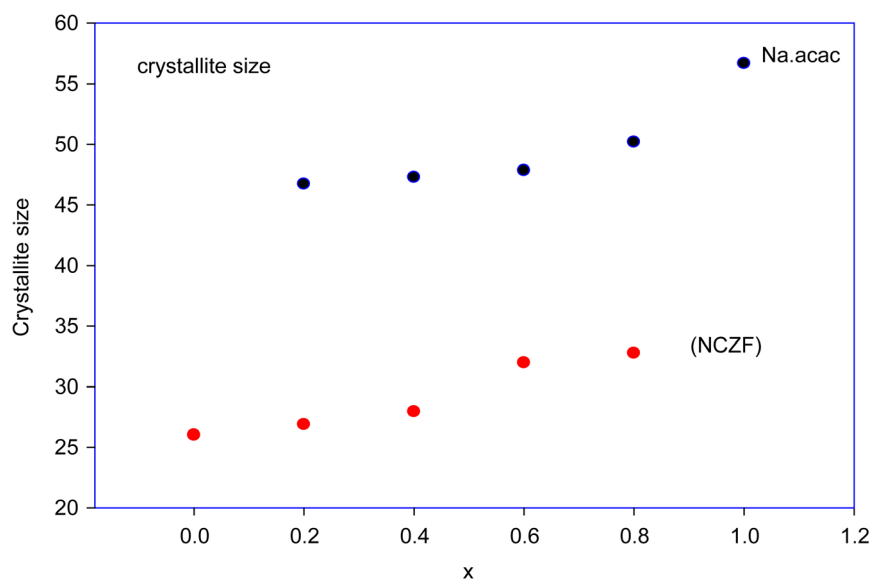


Figure 3. Crystallite size for composites $[(\text{NCZF})_{1-x} \text{Na}(\text{ac.ac})_x]$

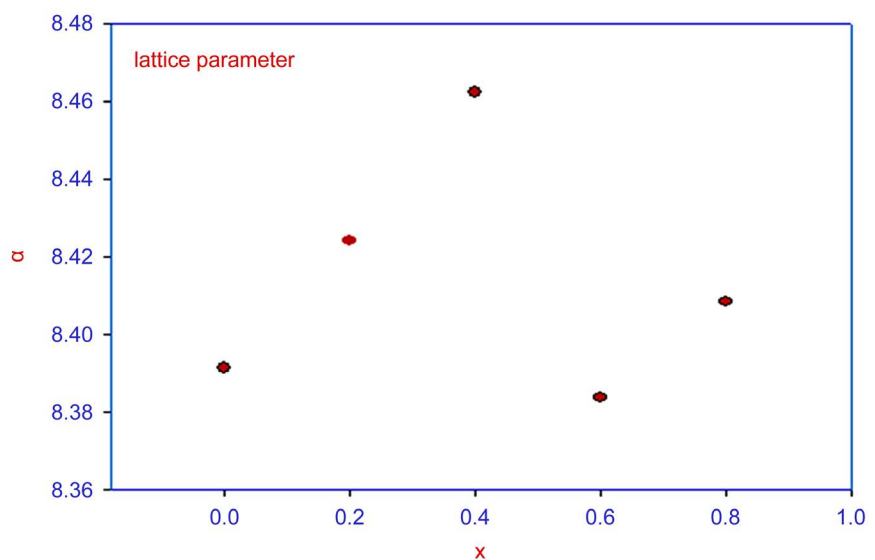


Figure 4. Lattice constant (a) as a function of Na(ac.ac) content.

The theoretical density and bulk density D_x , D of ferrite phase as a function of Na(ac.ac) content shown in **Figure 5**. It decreases by increasing Na(ac.ac) contents due to the lower density of Na(ac.ac) (2.1 g/m^3). The theoretical density D_x was calculated, and was higher than the bulk density due to the presence of pores. **Table 3** shows the mean ionic radius of the A- and B-sublattices (R_A and R_B) which can be calculated for $\text{Ni}_{0.45}\text{Co}_{0.2}\text{Zn}_{0.35}\text{F}_2\text{O}_4$ [NCZF] phase prepared by ceramic and co-precipitation method, using the cation distributions. The radius of octahedral site r_B and tetrahedral site r_A for (NCZF) for ferrite phase prepared by ceramic and co-precipitation method calculated by the relations [17]

$$r_A = 0.35r_{\text{Zn}} + yr_M + (0.65 - y)r_{\text{Fe}}$$

$$r_B = 1/2[(0.65 - y)r_M + (1.35 + y)r_{\text{Fe}}]$$

where r denotes to the ionic radius and y to the number of the $M = \text{Ni}^{2+}$ or Co^{2+} ions at the A-sites. The r_A and r_B for both sample have the same value depending on the cation distribution proposal. The expected cation distribution for a ferrite samples under consideration is given in the same table. The result confirmed that all the samples crystallize in the spinel structure irrespective the method of preparation. The as prepared sample by co-precipitation method has spinel phase without any calcination, which consider the successful process for preparation

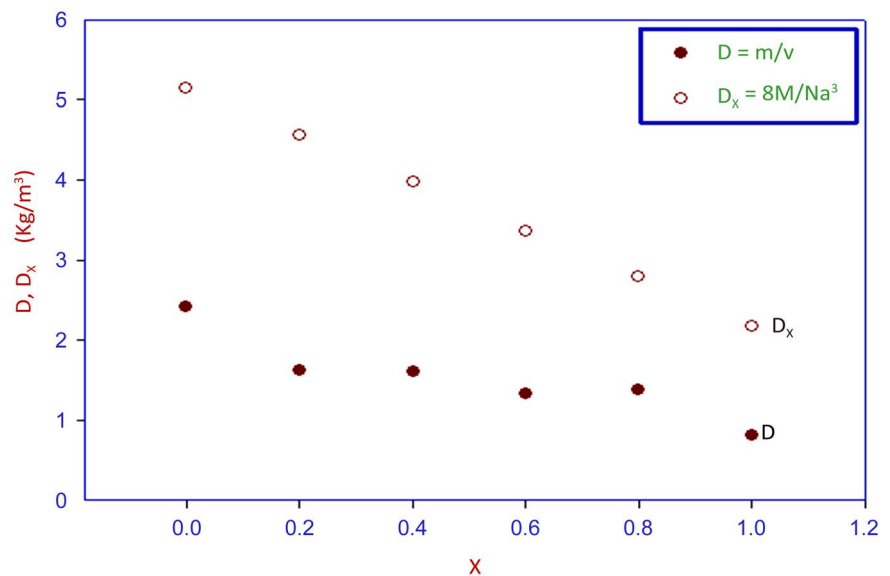


Figure 5. The theoretical density and bulk density D_x , D of ferrite phase as a function of Na(ac.ac) content.

Table 3. The radius of cathedral site R_B and tetrahedral site R_A for (NCZF) for ferrite phase prepared by Ceramic (S1) and Co-precipitation method (S2).

	A-site(nm)				B-site(nm)			R_A	R_B
	Zn	Co	Fe	Ni	Co	Fe			
S1	0.35	0.02	0.63	0.45	0.18	1.37	0.6798	0.6619	
S2	0.35	0.02	0.63	0.45	0.18	1.37	0.6798	0.6619	

of the ferrite sample. The Lattice parameter of the first sample (ceramic method) equal 8.4727 and for (co-precipitation method) equal 8.485, the broad peak of the sample (S1) indicate that crystallite size has lower value (25 nm) than that of S2 (36 nm).

3.2. Transmission Electron Microscopy (TEM)

Figure 6 shows that the transmission electron microscope photos of the composite samples prepared by co-precipitation method (as prepared) at different

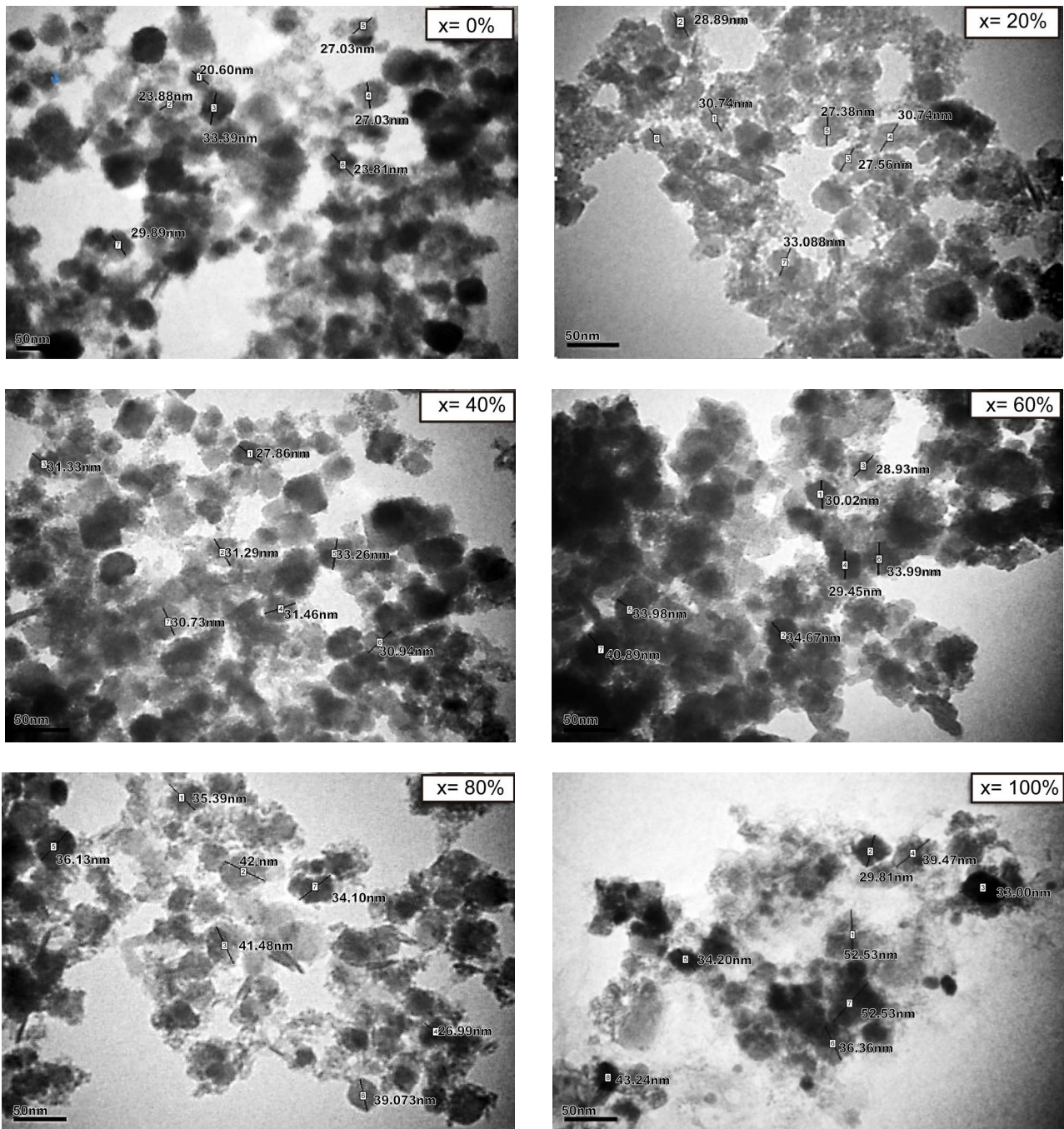


Figure 6. The TEM micrograph for the composite samples $[NCZF_{(1-x)} + Na(ac.ac)_{(x)}]$, $x = 0\%, 20\%, 40\%, 60\%, 80\%, 100\%$.

ratios of Na(ac.ac). It is apparent that the cubic nanoparticles diameter where ranged from (26 - 36 nm) and the particle size of Na(ac.ac) is greater than NCZF.

The analysis of TEM micrograph shows that the crystalline size was found to be in agreement with that obtained in XRD in **Table 4**. The same behavior has also confirmed from XRD beaks indicating polycrystalline nature of prepared sample. The size of the particles was observed to increase with Na(ac.ac) contents. The increase in crystalline size is most likely due to the agglomeration process of crystalline resulting in an increase in its size. We can conclude that the particle size may be controlled by either varying the annealing temperature of the sample or the addition Na(ac.ac) content. The crystallite size estimated from Scherrer's equation formula agrees well with that obtained from the corresponding TEM micrograph [18] [19].

Thus it is possible to control particle size by adjusting the ratio of Na.ac.ac content.

From TEM micrographs, the presence of Na(ac.ac) causes the repairing particles fused which lead to the increase of the particles size. Thus it is possible to control particle size by adjusting the ratio of Na(ac.ac) content

The TEM micrograph of ferrite nanoparticle synthesized by co-precipitation method and ceramic technique are shown in **Figure 7**. It is observed that the ceramic particle is slightly agglomeration and a particle size is higher than that of the co-precipitation method, moreover the ceramic particles are of irregular shape. This is evidence that the particle size of the co-precipitation method is smaller than these of the ceramic particles.

It is indicated from the TEM images that nanoparticles agglomerated for low value of Na(ac.ac) because of the isolation effect of Na(ac.ac) among the magnetic nanoparticle.

3.3. Scanning Electron Microscope (SEM) Micrograph Study

Figure 8 shows the surface morphologies of the as prepared nanoferrite prepared by co-precipitation method and the composite samples of $[\text{NCZF}_{(1-x)} + \text{Na}(\text{ac.ac})_x]$, $x = 0\%, 20\%, 40\%, 60\%, 80\%, 100\%$. It is illustrates that the grain size of NCZF is symmetrically and uniform. Two type grains appear at the composite sample one of them referred to NCZF and the other has needle shape

Table 4. The calculated crystallite sizes.

$[(\text{NCZF})_{1-x}(\text{Na}(\text{ac.ac}))_x]$	t (nm) from XRD	t (nm) from TEM
[100% (NCZF), 0% (Na(ac.ac))]	26.869	26.112
[80% (NCZF), 20% (Na(ac.ac))]	28.044	28.775
[60% (NCZF), 40% (Na(ac.ac))]	31.623	30.983
[40% (NCZF), 60% (Na(ac.ac))]	35.593	33.043
[20% (NCZF), 80% (Na(ac.ac))]	36.864	36.984
[0% (NCZF), 100% (Na(ac.ac))]	37.342	37.421

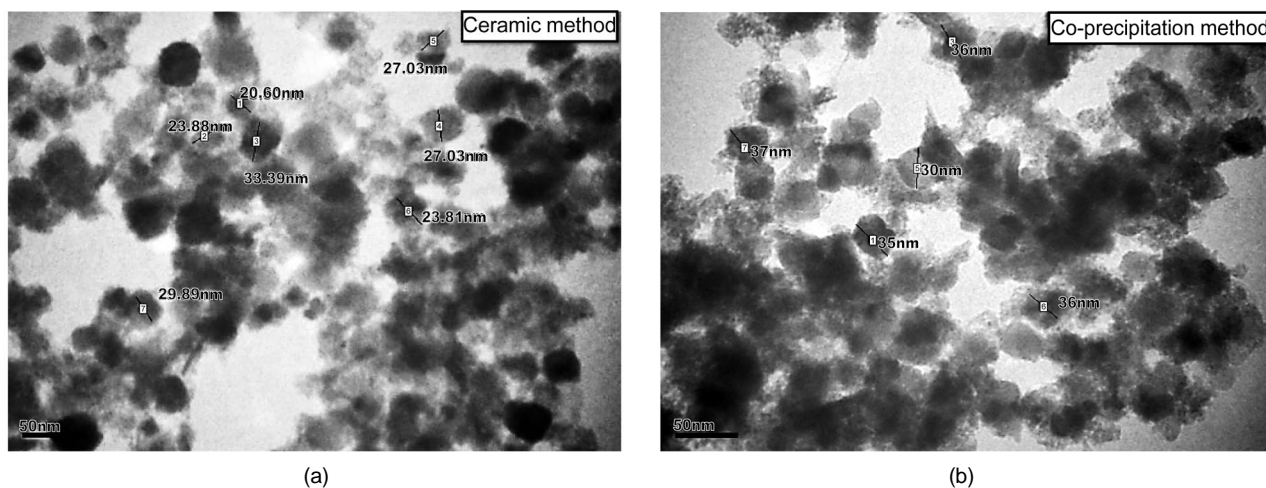


Figure 7. The comparison between the TEM micrographs NCZF nanoparticles prepared by (a) Ceramic method and (b) Co-precipitation method.

referred to Na(ac.ac). As seen in **Figure 8** the needle shape grains accumulate around the NCZF grains and become the predominant at higher content of Na(ac.ac). The grain size of NCZF increases by increasing Na(ac.ac) content. The presence of Na(ac.ac) enhances the grain growth which is varied from 0.1 - 3 μm . The microstructure of NCZF/a Na(ac.ac) composite has a very small pore with a good point contact. Finally we conclude that, ferrite grain growth has been enhanced when Na(ac.ac) exist as impurity phase [20] [21].

Figure 9 shows the SEM photograph for NCZF prepared by ceramic method at 1100°C for 4 hours; the average grain size estimated from micrograph was found $\approx 5 \mu\text{m}$. The influenced of sintering temperature in ceramic method on the grain growth is high enough to make the grain size of NCZF is greater than that prepared by co-precipitation method. It is difficult to obtain dense, homogenous and fine grains by solid-state reaction (ceramic method) because of the large difference between sintering behavior and thermal expansion coefficient of the constituents of ferrite.

Figure 9 describes the comparison between the SEM micrographs of the ferrite samples prepared by sintering process and co precipitation. The inhomogeneity of grain distribution in the sintered ferrite is shown as a good homogeneity of the grains in the ferrite prepared by co-precipitation method is also noticed giving rise to larger grain size of ceramic samples.

3.4. IR Spectral Analysis of the Composites

Figure 10 shows IR spectral analysis of single phase of ferrite and Na(ac.ac) and their composites. The spectra of ferroelectric phase has characteristic assigned band at 1010 cm^{-1} is due to the stretching vibration of (C-H) bond and the band at 866 cm^{-1} due to the binding vibration of (C-H) bond. The absorption band at 413 cm^{-1} is due to the (Na-C) bond vibration. On the other hand the appearance of IR absorption band near 3427 cm^{-1} is assigned to stretching vibration of (O-H) bond. The absorption band at 1507 cm^{-1} , 1614 cm^{-1} were assigned to (C=O) and

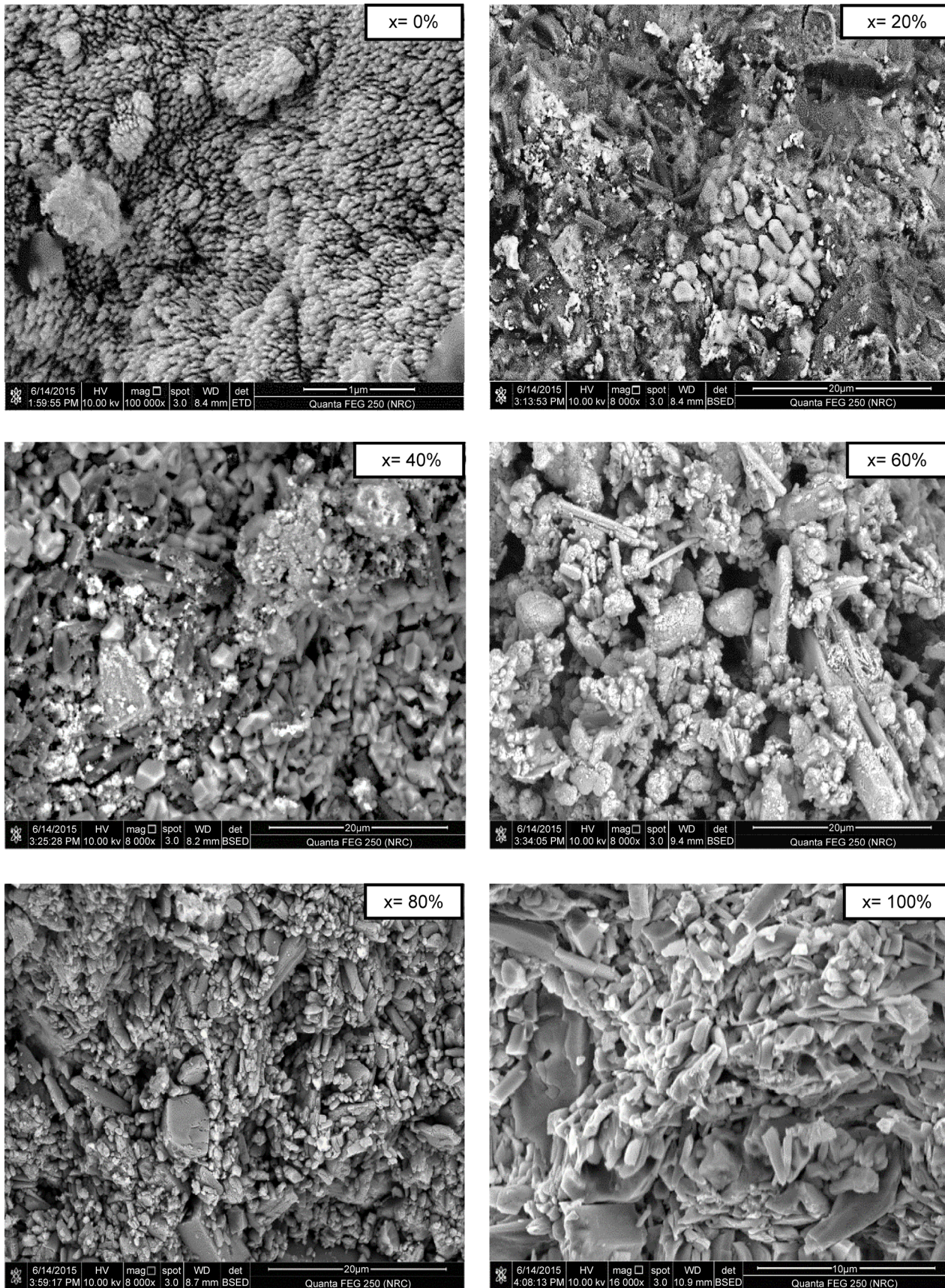


Figure 8. The SEM micrograph for the composite samples $[\text{NCZF}_{(1-x)} + \text{Na}(\text{ac.ac})_x]$, $x = 0\%$, 20% , 40% , 60% , 80% , 100% .

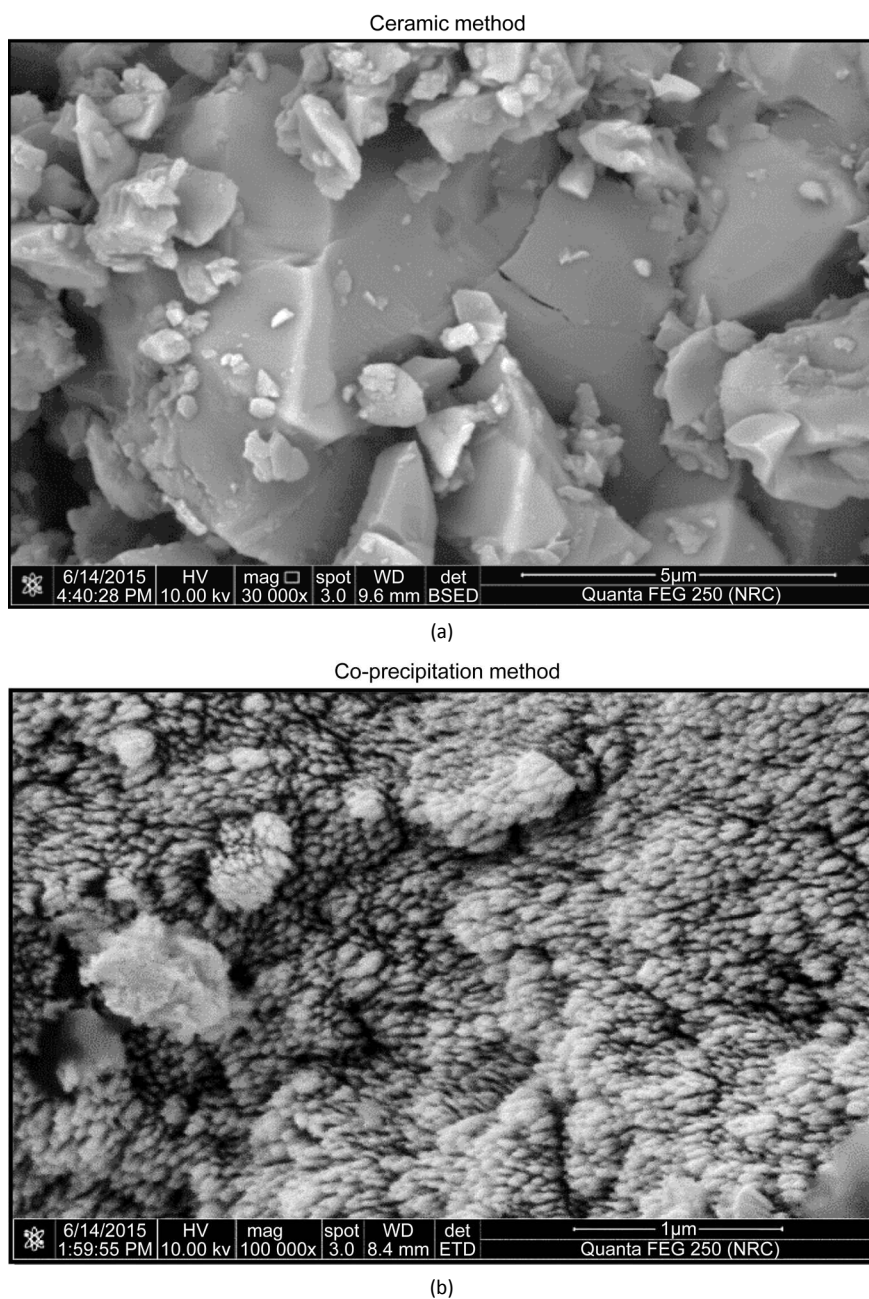


Figure 9. The comparison between The SEM micrographs NCZF nanoparticles prepared by (a) Ceramic method and (b) Co-precipitation method.

(C=C) stretching mode respectively. The intensities of these absorption bands decrease by increasing ferrite content and completely disappear at 100% ferrite. The two characteristic bands is at 590 and 419 cm^{-1} are due to stretching vibration of ($\text{Fe}^{3+}\text{-O}^{2-}$) bond at tetrahedral (ν_1) and octahedral (ν_2) mode of vibration. The characteristic absorption bands ν_1 and ν_2 values decreases by increasing Na(ac.ac) contents. This may be due to the shorting of Fe^{3+} bond length by introducing Na(ac.ac). **Figure 11** shows IR-spectra of ferrite samples prepared by ceramic and co-precipitation method. It appeared from the figure that the frequencies of characteristic band (ν_1) shift to higher frequency from 575 - 590 cm^{-1}

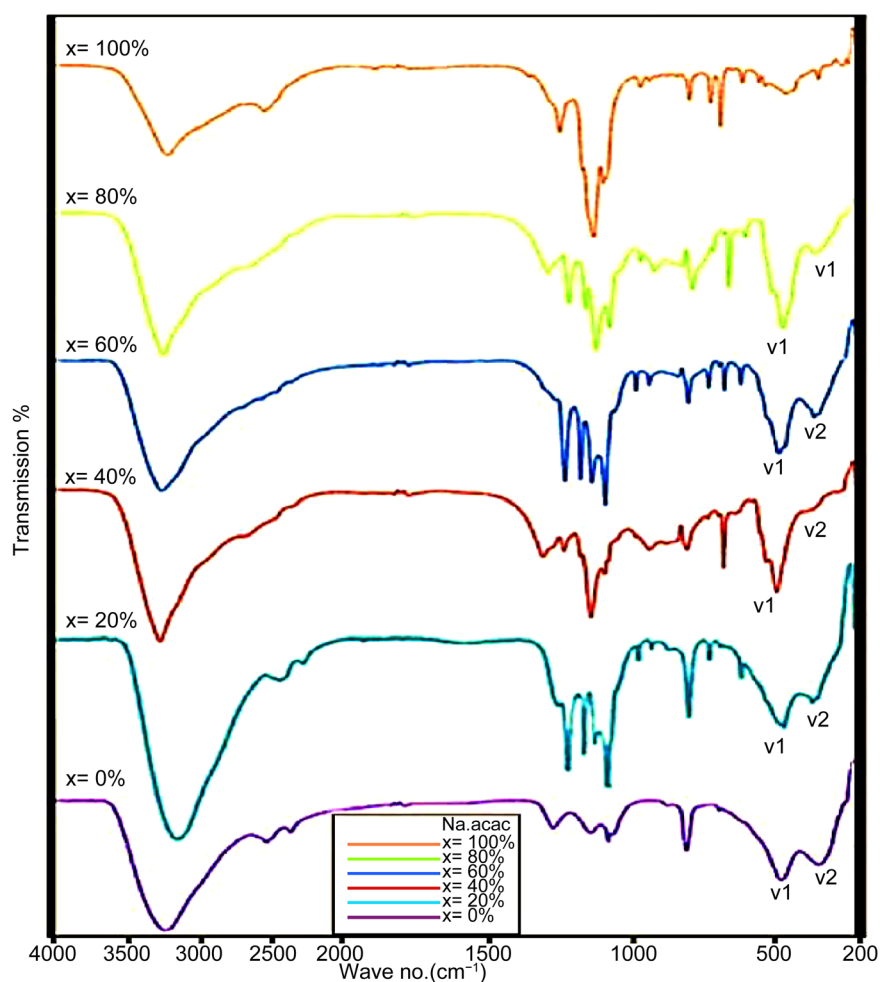


Figure 10. IR spectral for the nanocomposite samples $[\text{NCZF}_{(1-x)} + \text{Na}(\text{ac.ac})_{(x)}]$, $x = 0\%$, 20%, 40%, 60%, 80%, 100%.

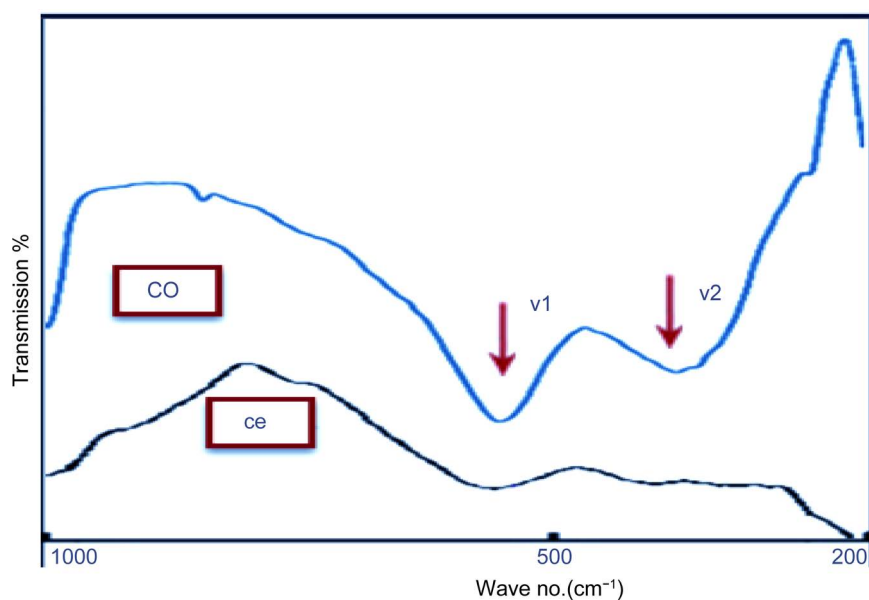


Figure 11. IR spectral for the nanocomposite $\text{Ni}_{0.45}\text{Co}_{0.2}\text{Zn}_{0.35}\text{F}_2\text{O}_4$ prepared by coprecipitation method (co) and ceramic method (ce).

Table 5. The force constant of both tetrahedral and octahedral increase by introducing Na(ac.ac).

x	$\nu_{\text{Tetra}}(\text{cm}^{-1})$	$F_{\text{Tetra}}(\text{dyne/cm})$	$\nu_{\text{Octa}}(\text{cm}^{-1})$	$F_{\text{Octa}}(\text{dyne/cm})$
0	590	255,620.027	419	128,919.585
0.2	568	236,912.254	435	138953.4608
0.4	569	237747.1867	433	137678.6651
0.6	601	247,028.375	459	132014.7833

for ν_1 and nearly constant for ν_2 . These results show the preparation method affect the molecular character of ferrite [20].

Since of the vibrational frequencies are proportional to the force constant according to the formula [22]

$$F = 4\pi^2 \nu^2 c^2 \mu$$

where, c is velocity of light, ν is frequency band and μ is reduced mass of ($\text{Fe}^{3+}\text{-O}^{2-}$).

The force constant of both tetrahedral and octahedral increase by introducing Na(ac.ac) as given in Table 5. This mean that the electronic distribution of (Fe-O) bond is greatly affected by the addition of Na(ac.ac) which causing change of electric dipole moment of this bond. In conclusion, the presence of Na(ac.ac) effect of inter molecular character of ferrite. The difference between the two characteristic frequencies ν_1 and ν_2 is about 171 cm^{-1} for pure ferrite and decreases by increasing Na(ac.ac) and reaches to 141 cm^{-1} for 60% Na(ac.ac). These indicate that the ratio of ferrimagnetic phase decreased by introducing the ferroelectric phase.

4. Conclusion

The addition (Na(ac.ac)) has considerable effect on crystalline morphology structure of both ferrite and (Na(ac.ac)). The average crystallite size of both phases increases by increasing (Na(ac.ac)) content whereas the value of crystallite size of Na(ac.ac) is higher than that of ferrite phase. Density of ferrite decreases by increasing Na(ac.ac) contents due to the lower values of Na(ac.ac) density (1 kg/m^3). It is evidence that the coprecipitation method gives ferrite particle smaller size than the ceramic particles and the inhomogeneity of grain distribution in the sintered ferrite, whereas good homogeneity of the grains in the ferrite is prepared by coprecipitation method. The addition of Na(ac.ac) may change the molecular character of ferrite leading to the change of band frequency.

References

- [1] Shen, J.H., Bai, Y., Zhou, J. and Li, L.T. (2005) Magnetic Properties of a Novel Ceramic Ferroelectric-Ferromagnetic Composite. *Journal of the American Ceramic Society*, **88**, 3440. <https://doi.org/10.1111/j.1551-2916.2005.00633.x>
- [2] Qi, X., Zhou, J., Li, B., Zhang, Y., Yue, Z., Gui, Z. and Li, L.T. (2004) Preparation and Spontaneous Polarization-Magnetization of a New Ceramic Ferroelectric-Fer-

- romagnetic Composite. *Journal of the American Ceramic Society*, **87**, 1848-1852.
<https://doi.org/10.1111/j.1151-2916.2004.tb06329.x>
- [3] Kanai, T., Ohkoshi, S., Nakajima, A., Watanabe, T. and Hashimoto, K. (2001) A Ferroelectric Ferromagnet Composed of $(\text{PLZT})_x(\text{BiFeO}_3)_{1-x}$ Solid Solution. *Advanced Materials*, **13**, 487-490.
[https://doi.org/10.1002/1521-4095\(200104\)13:7<487::AID-ADMA487>3.0.CO;2-L](https://doi.org/10.1002/1521-4095(200104)13:7<487::AID-ADMA487>3.0.CO;2-L)
- [4] Dong, L.Y., Du, P.Y. and Weng, W.J. (2007) Effect of Phase Formation on Magnetism of Sol-Gel Derived $\text{PbTiO}_3/(\text{Ni, Pb})$ Ferrite Composite Powders. *Key Engineering Materials*, **336-338**, 706-708.
<https://doi.org/10.4028/www.scientific.net/KEM.336-338.706>
- [5] Rontgen, W.C. (1888) Ueber die durch Bewegung eines im homogenen electrischen Felde befindlichen Dielectricums hervorgerufene electrodynamische Kraft. *Annales de Physique*, **35**, 264-270. <https://doi.org/10.1002/andp.18882711003>
- [6] Curie, P. (1894) On symmetry in Physical Phenomena. *Journal de Physique*, **3**, 393.
- [7] Valasek, J. (1920) Piezoelectric and Allied Phenomena in Rochelle Salt. *Physical Review*, **15**, 537-538.
- [8] Fox, D.L. and Scott, J.F. (1977) Ferroelectrically Induced Ferromagnetism. *The Journal of Physical Chemistry C*, **10**, L329-L331.
- [9] Pecharroman, C. (2000) Experimental Evidence of a Giant Capacitance in Insulator-Conductor Composites at the Percolation Threshold. *Advanced Materials*, **12**, 294-297.
[https://doi.org/10.1002/\(SICI\)1521-4095\(200002\)12:4<294::AID-ADMA294>3.0.CO;2-D](https://doi.org/10.1002/(SICI)1521-4095(200002)12:4<294::AID-ADMA294>3.0.CO;2-D)
- [10] Goodarzi, A., Sahoo, Y., Swihart, M.T. and Presad, P.N. (2004) Aqueous Ferrofluid of Citric Acid Coated Magnetite Particles. *Materials Research Society Symposium Proceedings*, **789**, N6. 6.1.
- [11] Racuciu, M., Creanga, D.E. and Calugaru, Gh. (2005) Synthesis and Rheological Properties of an Aqueous Ferrofluid. *Journal of Optoelectronics and Advanced Materials*, **7**, 2859-2864.
- [12] Charles, G. (1963) Tetraacetylene. *Organic Syntheses*, **4**, 869-871.
- [13] Hemed, O.M., Ayad, M.I., Heneshand, M.A. and Abo Sekkina, M.M. (1994) Thermoelectric and Dielectric Investigations of the Thermochromism of Various *n*-Acetylacetonate Phases and Intermediates. *Phase Transitions*, **48**, 207-215.
- [14] Sawaby, A.Z. (1971) PhD Thesis, Cairo University, Giza.
- [15] Reddy, P. and Salagram, M. (1987) The Far-Infrared Spectra of Mixed Manganese-Magnesium Ferrites. *Physica Status Solidi (A)*, **100**, 639-643.
<https://doi.org/10.1002/pssa.2211000230>
- [16] Singh, R.K., Upadhyay, C., Layek, S. and Yadav, A. (2010) Cation Distribution of $\text{Ni}_{0.5}\text{Zn}_{0.5}\text{Fe}_2\text{O}_4$ Nanoparticles. *International Journal of Engineering, Science and Technology*, **2**, 104-109.
- [17] Godake, J.S., Kambale, R.C., Salvi, S.V., Sawant, S.R. and Suryavanshi, S.S. (2009) Electric Properties of Co Substituted Ni-Zn Ferrites. *Journal of Alloys and Compounds*, **486**, 830-834.
- [18] Sualka, O., Sarma, R.K., Sebastian, V., Lakshmi, N. and Venugopalan, K. (2007) A Study of Nanosized Ni Substituted Co-Zn Ferrite Prepared by Coprecipitation. *Journal of Magnetism and Magnetic Materials*, **313**, 198-203.
- [19] Li, L., Peng, L., Hua, X. and Yang, D. (2012) Effect of Cu and Co Substitution on the Preparation of NiZn Ferrite Thin Films. *Journal of Electronic Science and Technology*, **10**, No. 1.

- [20] Ling, W., Zhang, H., Li, Y. and Wang, Y. (2011) Magnetic and Dielectric Properties of Low Temperature Fired Ferrite/Ceramic Composite Material. *Material International*, **21**, 21-26
- [21] Shaikh, P.A., Kambale, R.C., Rao, A.V. and Kolekar, Y.D. (2010) Structural, Magnetic and Electrical Properties of Co-Ni-Mn Ferrites Synthesized by Co-Precipitation Method. *Journal of Alloys and Compounds*, **492**, 590-596.
<https://doi.org/10.1016/j.jallcom.2009.11.189>
- [22] Mazen, S.A., Zaki, H.M. and Mansour, S.F. (2007) Infrared Absorption and Dielectric Properties of Mg-Zn Ferrite. *International Journal of Pure and Applied Physics*, **3**, 40-48



Scientific Research Publishing

Submit or recommend next manuscript to SCIRP and we will provide best service for you:

Accepting pre-submission inquiries through Email, Facebook, LinkedIn, Twitter, etc.

A wide selection of journals (inclusive of 9 subjects, more than 200 journals)

Providing 24-hour high-quality service

User-friendly online submission system

Fair and swift peer-review system

Efficient typesetting and proofreading procedure

Display of the result of downloads and visits, as well as the number of cited articles

Maximum dissemination of your research work

Submit your manuscript at: <http://papersubmission.scirp.org/>

Or contact ojapps@scirp.org

